

Reverse Phase Separation of Phospholipids Incorporating Piperidine As A Post Column Modifier for Negative Ion Detection by Mass Spectrometry

Cory A. Lytle, Yingdong M. Gan and David. C. White

Center for Environmental Biotechnology, University of Tennessee, 10515 Research Drive, Suite 300, Knoxville, TN 37932-2575, USA
 CLytle@utk.edu Mgan@utkux.utcc.utk.edu MILipids@aol.com

Summary

The objective of this method is to provide a rapid and sensitive analysis for the detection and identification of phospholipids by High Performance Liquid Chromatography/Electrospray Ionization/Mass Spectrometry (HPLC/ESI/MS). Phospholipids make up a major part of cell membranes and their metabolic lability to endogenous and exogenous phospholipase make them excellent indicators for viability in determination of biomass¹, active community composition², nutritional/physiological status³, and in defining end points for bioremediation⁴. These phospholipids contain acyl groups at the *sn*-1 and *sn*-2 position while possessing a polar head group containing a phosphate group at the *sn*-3 position. The two acyl groups can range from saturated, cyclic, hydroxy, to unsaturated fatty acids. The nature of these acyl groups along with the polar head group is used in the determination of the microbial community structure. **Figure 1** shows the structure of glycerophospholipid along with the polar head groups of interest.



Figure 1. Structure of glycerophospholipid and polar head groups of interest

Experimental

Samples. Glycerophospholipid standards, PG (P0514), PE (P9137), and PC (P6638) were purchased from Sigma (St. Louis, MO). Standards were prepared at 10 ppm in methanol and diluted accordingly. All solvents were HPLC grade. Water was obtained from an in-house source of Millipore water (Millipore, Bedford, MA).

HPLC. Separation of the glycerophospholipids was carried out on an HP 1100 HPLC (Agilent, Sunnyvale, CA) using a microbore C18 column (Higgins Analytical, Mountain View, CA). **Table 1** shows the column parameters. The post column modifier was incorporated by a Harvard "33" Dual Syringe Pump (Harvard Apparatus, Holliston, MA).

Mass Spectrometry. Electrospray mass spectra were obtained using both a VG Platform II single quadrupole MS and a VG Quattro II triple quadrupole MS. Instrument tuning was performed utilizing a synthetic PG standard. Calibration of the Platform II was performed in the negative ion mode with a solution of sodium iodide/cesium iodide. Samples were introduced into the Platform II ESI source at a total flow rate of 60 $\mu\text{L}/\text{min}$. The electrospray capillary was operated at -2.78 kV. The counter electrode was operated at 0.41 kV. The cone was set to -80 V, while the skimmer lens offset was set to 5 V. The source was operated at 80°C . The calibration of the Quattro II was performed using a solution of horse heart myoglobin in the positive ion mode. Samples were infused into the Quattro II at a flow rate of 20 $\mu\text{L}/\text{min}$. Capillary voltage was optimized at 2.5 kV, counter electrode at 0.50 kV, cone at -80 V and skimmer lens offset to 5 V. The source was operated at 80°C . The collision energy was optimized at 45 V and the collision cell gas pressure was set to 3.7×10^{-3} mbar. The collision gas was argon.

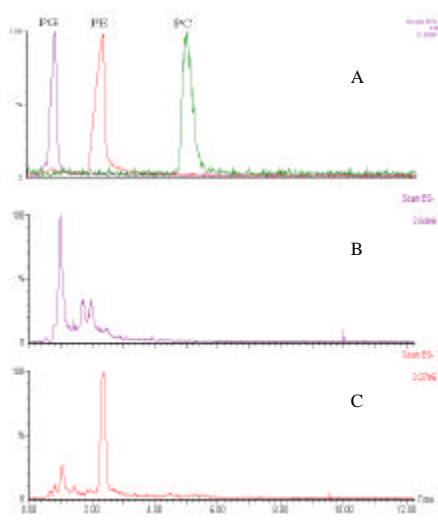


Figure 2. (A) Class separation of glycerophospholipids. (B) EIC for PG from soil sample. (C) EIC for PE from soil sample.

Column	HAISIL HL C18 3 μm , 30 mm x 1 mm
Mobile phase	95/5 (MeOH + 0.002% piperidine/H ₂ O, v/v)
Column flow rate	50 $\mu\text{L}/\text{min}$
Column temperature	27°C
Post column modifier	0.02% piperidine in MeOH, v/v
Post column modifier flow rate	10 $\mu\text{L}/\text{min}$

Table 1. HPLC column parameters.

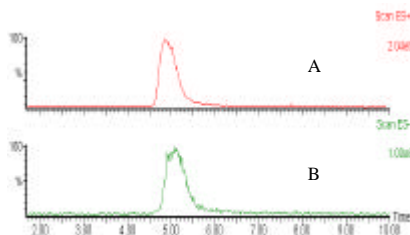


Figure 3. (A) EIC for PC in positive ion mode. (B) EIC for PC in negative ion mode

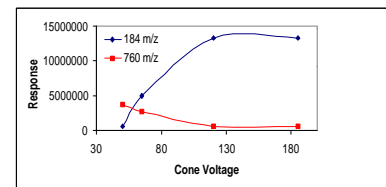


Figure 4. Ion abundance of m/z 760 and m/z 184 of PC at increasing cone voltages.

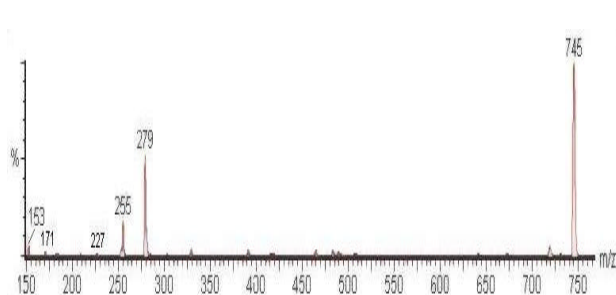


Figure 5. ESI mass spectrum of 1-palmitoyl-2-linoleoyl-sn-glycero-3-phosphatidylglycerol.

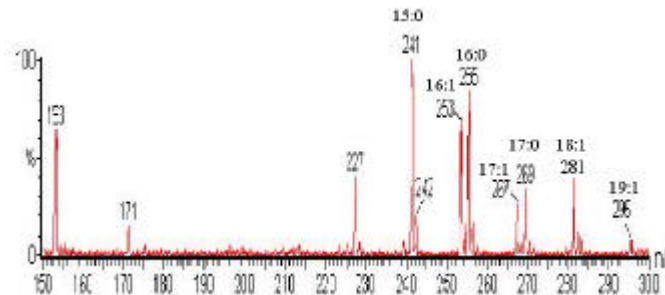


Figure 6. ESI spectrum for PG shown in figure 2B, long with corresponding fatty acids.

m/z	Corresponding ion
153	$[\text{CH}_2\text{C}(\text{OH})\text{CH}_2\text{HPO}_4]^-$
171	$[\text{HPO}_4\text{CH}_2\text{CH}(\text{OH})\text{CH}_2\text{OH}]^-$
227	$[\text{CH}_2\text{C}(\text{OH})\text{CH}_2\text{PO}_4\text{CH}_2\text{CH}(\text{OH})\text{CH}_2\text{OH}]^-$
255	$[\text{CH}_3(\text{CH}_2)_{14}\text{COO}]^-$
279	$[\text{CH}_3(\text{CH}_2)_9\text{CHCHCH}_2\text{CHCH}(\text{CH}_2)_2\text{COO}]^-$
745	$[\text{M}-\text{H}]^-$

Table 2. ESI negative ions characteristic of PG and the two acyl substituents in figure 5.

Head Group	m/z	Corresponding ion
PG	153	$[\text{CH}_2\text{C}(\text{OH})\text{CH}_2\text{HPO}_4]^-$
	171	$[\text{HPO}_4\text{CH}_2\text{CH}(\text{OH})\text{CH}_2\text{OH}]^-$
	227	$[\text{CH}_2\text{C}(\text{OH})\text{CH}_2\text{PO}_4\text{CH}_2\text{CH}(\text{OH})\text{CH}_2\text{OH}]^-$
PE	140	$[\text{HPO}_4\text{CH}_2\text{CH}_2\text{NH}_2]^-$
	196	$[\text{CH}_2\text{C}(\text{OH})\text{CH}_2\text{PO}_4\text{CH}_2\text{CH}_2\text{NH}_2]^-$
PC	168	$[\text{HPO}_4\text{CH}_2\text{CH}_2\text{N}^+(\text{CH}_3)_2]^-$
	224	$[\text{CH}_2\text{C}(\text{OH})\text{CH}_2\text{PO}_4\text{CH}_2\text{CH}_2\text{N}^+(\text{CH}_3)_2]^-$

Table 3. Low mass ions diagnostic of polar head groups of PG, PE, and PC.

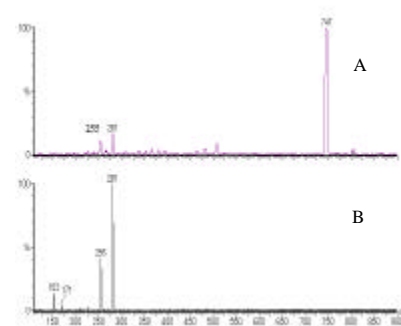


Figure 7. (A) ESI spectra for 1 ppm PG 16:0/18:1 when scanning from m/z 110-900. (B) ESI product ion spectra for m/z 747 of 1 ppm PG 16:0/18:1 when scanning from m/z 110-900.

Conclusions

A class separation of glycerophospholipids, phosphatidylglycerol (PG), phosphatidylethanolamine (PE), and phosphatidylcholine (PC) was performed on a microbore C18 column by reversed phase HPLC. The mobile phase consisted of 95% methanol and 5% water. The analysis was complete in less than 10 minutes (Figure 2A). Electrospray ionization (ESI) was used to transfer the ions present in solution to the gas phase. When acquiring data with a single quadrupole instrument, features of the up-front CID spectra are dependant upon the sampling cone voltage. When a high cone voltage was applied, a weak, singly charged $[\text{M}-\text{H}]^-$ ion was observed whereas ions diagnostic of the two acyl substituents and the polar head group intensify. When the cone voltage was decreased, unfragmented parent ions were collected as ions diagnostic of the two acyl substituents and polar head group are absent. PC was best detected in the positive ion mode due to the positively charged quaternary nitrogen in the head group (Figure 3). Figure 4 shows the ion abundance of two distinct positive ions of PC, 760 m/z $[\text{M}+\text{H}]^+$ and 184 m/z corresponding to the polar head group $[\text{H}_2\text{PO}_4\text{CH}_2\text{CH}_2\text{N}(\text{CH}_3)_3]^+$ as the cone voltage is ramped. At low cone voltages the higher mass ion was most abundant, whereas at high cone voltages, the ion at m/z 184 was most prominent. Figure 5 shows the ESI mass spectrum for PG containing 16:0 and 18:2 fatty acids. Note the relative intensity of the sn1 fatty acid roughly a third of the sn2. This can be used to determine the positional specificity. Table 2 shows the ESI negative ions characteristic of PG and the two acyl substituents in figure 5. This analysis was tested on actual samples from an environmental matrix. Figure 2B shows an EIC for ions diagnostic of PG from the soil sample, while Figure 2C shows an EIC for ions diagnostic of PE from the soil sample. The spectrum for the peak at 1.0 minute in figure 2B is shown in Figure 6 along with the associated fatty acids. Ions were detected in the negative ion mode by incorporating piperidine as a post column modifier. Piperidine (hexahydropyridine), $\text{C}_5\text{H}_{11}\text{N}$ is a strong base (pK at 25°C = 2.8) which works well to deprotonate analytes of interest. The piperidine would also compete for active sites thus making the tailing of the PE's less noticeable. Because the polar head groups are different, low mass ions diagnostic of each polar head group can also be identified (Table 3). Product ion scans were also performed to compare the sensitivity between the single quadrupole and the triple quadrupole instrument. Figure 7A shows the ESI mass spectrum for 1 ppm PG 16:0/18:1 when scanning from m/z 110-900. Figure 7B shows the ESI product ion spectrum for m/z 747 of 1 ppm PG 16:0/18:1 when scanning from m/z 110-900. The product ion spectrum is approximately 50x more sensitive. Limits of detection (LOD) and limits of quantitation (LOQ) were experimentally determined to be 20 fmol/ μL and 60 fmol/ μL respectively when acquiring data in the selected ion recording (SIR) mode monitoring three ions with a single quadrupole MS. When acquiring data from m/z 110-900 in the scanning mode, the LOD and LOQ were experimentally determined to be 1 pmol/ μL and 3 pmol/ μL . When acquiring product ion spectra for m/z 747, the LOD and LOQ were experimentally determined to be 446 attomol/ μL and 1.3 fmol/ μL , respectively.

Acknowledgements

This work was supported by National Science Foundation grant DEB 9814813 and the Department of Energy, Office of Energy Research, grant number DE-FC02-96ER62278White (part of the Assessment Component of the Natural and Accelerated Bioremediation Research Program, NABIR). The authors also wish to thank Dr. Al Tuinman of the Mass Spectrometry Facility at The University of Tennessee, Department of Chemistry, for the use of the Quattro II.

References

- Ringelberg, D. B., S. Sutton, and D. C. White 1997. Biomass bioactivity and biodiversity: microbial ecology of the deep subsurface: analysis of ester-linked fatty acids. *FEMS Microbiology Reviews* 20: 371-377
- White, D. C., J. O. Stair, and D. B. Ringelberg. 1996. Quantitative Comparisons of *in situ* Microbial Biodiversity by Signature Biomarker Analysis. *J. Indust Microbiol.* 17, 185-196.
- White, D. C. 1995. Chemical ecology: Possible linkage between macro- and microbial ecology. *Oikos*, 74, 174-181.
- White, D. C., C. A. Flemming, K. T. Leung, and S. J. Macnaughton. 1998. *In situ* microbial ecology for quantitative appraisal, monitoring, and risk assessment of pollution remediation in soils, the subsurface and in biofilms. *J. Microbiol. Methods*, 32, 93-105.